# CHAPTER III

## EXPERIMENTAL PARAMETERS OF THE MÖSSBAUER EFFECT

### 1. Sources and Absorbers.

Even though some of the Mössbauer candidates have a potentially narrower line than $^{57}Fe$, the latter is still the best source for precision experiments as it not only exhibits near natural line widths, but has also a large recoilless fraction at room temperature depending on the host lattice used.

The ideal host lattice would have a cubic symmetry and be diamagnetic with the impurity atoms tightly bound at equivalent lattice sites. This would ensure that there would be no quadrupole or magnetic splitting and that the isomeric shift would be constant.

Even if such materials were available for various Mössbauer nuclei, the practical problem of ensuring uniform conditions throughout the lattice and incorporating the source and absorber at equivalent sites remains. Taking the example of a natural iron foil absorber, which comes nearest to exhibiting a natural line width (Kerler, et al., 1962; Housley, et al., 1964), one can broaden the observed line width by as much as $\Gamma$ by introducing dislocations and imperfections in the absorber foil (Abou-Elnasr, 1968). The line width can then be brought back to its original value by annealing the absorber for several hours in a reducing atmosphere, which would eliminate the strain in the foil and reduce the imperfections.

Using various transition metals as the host lattice for the source and a sodium ferrocyanide absorber, line widths have been obtained that range from .28 mm/sec to .60 mm/sec (Qaim, 1965) with Pd and Cu giving the narrowest lines. Also the metals

with a f.c.c. structure give generally a narrower line than those with a b.c.c. symmetry. This illustrates that the impurity atoms are better incorporated in some metals than in others, even though the crystal structure may be the same. In these studies no recipe has been found for obtaining narrow source and absorber lines. This does not of course preclude the possibility of finding some host material that does give rise to natural line width for the other narrow line Mössbauer sources.

The potential competitors to $^{57}$Fe are $^{73}$Ge (13.5 keV) and $^{181}$Ta (6.25 keV), where both, because of the small transition energy, should have a recoilless fraction comparable to or larger than that of $^{57}$Fe. The problem with $^{73}$Ge is that it has a large internal conversion coefficient, $\alpha \sim 1300$ (Czjzek, et al., 1965) so that no effect has as yet been observed, and in any case, the large internal conversion coefficient would severely limit the practical use of the line in high precision experiments.

$^{181}$Ta is a more hopeful possibility. A 5% resonant effect has been observed (Steyert, et al., 1965) but the resultant line width was 1.0 mm/sec instead of the expected .007 mm/sec. This excessive broadening was attributed to quadrupole splitting arising from the very large electric quadrupole moment of the nucleus where the resulting sensitivity to electric field gradients is ~ 700 times larger than it is for $^{57}$Fe.

For the present work $^{57}$Fe was used throughout. To obtain the highest sensitivity, the source and absorber had to satisfy several criteria:

(i) large recoilless fraction,

(ii) unsplit line of near natural width,

(iii) optimum shift between source and absorber,

(iv) small electronic absorption,

(v) optimum absorber thickness.

The following sections discuss the problem of measuring and optimizing some of these parameters.

2. Transmission Spectra.

For large resonance effects a transmission geometry is most suitable, as it utilizes most of the source radiation. A transmission spectrum is then obtained by correlating the number of gamma rays detected with the Doppler velocity used to scan the emission line over the absorption line (or vice versa). The resonance will show up as a dip in the transmission spectrum, which is referred to as negative detection.

An alternative method is to detect the associated X-rays or electrons produced by the internal conversion process in $\frac{a}{1+a}$ of the gamma rays absorbed. This is known as positive detection because the counting rate at resonance will be increased. The relative merit of each system depends on the detection geometry, the source strength, and the detector used.

A kick sorter with 128 channels and a double Goodman's vibrator were used to obtain the velocity spectra. The motion device and associated equipment have been described previously (Isaak, 1965). As the vibrator could be fed with a variety of velocity waveforms, the system allowed for a ready determination of the resonance dip, line width, shift, and background.

2.1 Background Correction.

Even though the resolution of the detector, in this case usually a proportional counter, is of the order of 15% the degraded high energy gamma rays usually still contribute around 20% to the counting rate under the 14.4 keV peak. This contribution can be accurately determined by measuring the residual counting rate after interposing a 1/8" aluminum sheet in the source beam which effectively eliminates the low energy gamma rays and reduces the high energy gamma rays by a known amount.

2.2 Resonance Dip.

For an unshifted line the resonance dip $R_m$ is determined by comparing the counting rates at resonance $\dot{N}(0)$ and off resonance $\dot{N}(\infty)$ corrected for the background counting rate $\dot{N}_{BG}$.

$$R_m = \frac{\dot{N}(\infty) - \dot{N}(0)}{\dot{N}(\infty) - \dot{N}_{BG}}$$

$\dot{N}(\infty)$ was obtained using a square wave to drive the source at a few mm/sec. In the presence of a shift, the relative counting rates were most readily determined from the full transmission spectrum.

2.3 Transmission Line Width.

To economize on the accumulation time, the velocity of the vibrator is best adjusted to sweep over ~ 4 transmission line widths. Then correcting the counting rate at the wings to obtain the true off-resonance counting rate, a correction at the 2% level (see Section 3.3), one can directly determine the full line width at half the minimum $\Gamma_{\exp}$.

To calibrate the width, another spectrum is taken with an iron absorber where the inner two lines are split by 1.667 mm/sec.

2.4 Shift.

Two methods are available to measure the shift, depending on the desired accuracy. The shift can be deduced from the transmission spectrum knowing the channel corresponding to zero velocity. That channel is found by taking another spectrum in which the velocity of the vibrator has been reversed.

A more accurate measurement of the shift can be made if one concentrates on 3 (or 4) points of the resonance line to improve the statistical accuracy of each. Then if the normalized accumulated counts at velocities $V_1$, $V_2$, $V_3$ are $N_1$, $N_2$, $N_3$ the shift will be (Wilson, 1966)

$$\Delta E(\text{mm/sec}) = \frac{1}{2}\left( V_1 + V_2 + \frac{N_1 - N_2}{N_3 - N_2}(V_3 - V_2) \right)$$

$$\text{with } \sigma^2(V) = \frac{(V_3 - V_2)^2}{4(N_3 - N_2)^4}\Big[(N_3 - N_2)^2 \dot{N}_1 + (N_3 - N_1)^2 \dot{N}_2 + (N_1 - N_2)^2 \dot{N}_3\Big]$$

where $V_1$ lies on one side of the steepest part of the resonance and $V_2$ and $V_3$ on the other.

3. Transmission Intensity.

A number of authors have investigated the problem of how the absorption line width is affected by the thickness of the source and absorber. Margulies, et al., and more recently Heberle (1968) have studied the case of unbroadened source and absorber lines, and O'Connor (1963) has treated the case of Lorentz broadened lines.

## 3.1 Unbroadened Emission and Absorption Lines $\Gamma_s$, $\Gamma_a$.

The source radiation consists of a fraction $f_S$ emitted without recoil, which is subject to nuclear and electronic absorption, and the remaining fraction emitted with recoil attenuated only by electronic absorption. For an unsplit thin source; i.e., one that does not exhibit self-absorption, the emitted intensity is:

$$I(E^l)dE = In(E^l)dE + I_r(E^l)dE$$
$$= \frac{f_s \Gamma dE}{2\pi\left[(E^l - E_\circ)^2 + \left(\frac{\Gamma}{2}\right)^2\right]} + \frac{(1-f_s)dE}{kT} \qquad \text{... 3.1}$$

where $E^l = E + S$ and $S$ is the first order Doppler shift $\frac{vE_\circ}{c}$. The first term represents the unshifted natural line, and the second term is an approximate expression for the thermally broadened line where both contributions are normalized to unity.

The absorption cross-section per unit thickness of absorber will exhibit a similar dependence

$$\sigma(E) = \frac{\sigma_\circ n f_a \Gamma^2}{4\left[(E - E_\circ)^2 + (\Gamma/2)^2\right]} + \sigma = C_n(E) + \sigma_e \qquad \text{... 3.2}$$

where n is the number of resonant nuclei per unit thickness, $f_a$ is the recoilless fraction of the absorber, $\sigma_\circ$ is the peak absorption cross-section, and $\sigma_e$ denotes the electronic absorption cross-section. The resulting intensity using an unsplit absorber of thickness it will be:

$$N(E^l) = (1-f_s)e^{-t\sigma_e} + e^{-t\sigma_e}\int_\circ^\infty I_n(E^l)e^{-t\sigma_n(E)}dE \qquad \text{... 3.3}$$

This expression can be correlated with the experimentally determined $R_m$ value by defining

$$R(S) = \frac{N(\infty) - N(E^l)}{N(\infty)} \qquad \text{... 3.4}$$
$$= f_s(1 - \int I_n(E^l) e^{-\sigma n(E) t} dE)$$

For $E^l = E_\circ$ this becomes

$$R(0_l T_a) = f_s(1 - e^{-T_a/2} J_\circ(\frac{iTa}{2})) \qquad \text{... 3.5}$$

where $T_a = ntf_a\sigma_\circ = Nf_a\sigma_\circ$

Expression 3.3.4 has been evaluated numerically assuming that the transmission spectrum is Lorentzian (Boyle and Hall, 1962)

$$R(S, T_a) = \frac{R(0, T_a)}{1 + (2S/\Gamma_t)^2} \text{ for } 0 < T_a < 5 \qquad \text{... 3.6}$$

where

$$\Gamma_t(T_a) = 2\Gamma(1 + 0.135 T_a) \text{ (Visscher 1961)} \qquad \text{... 3.7}$$

$R(S, T_a)$ and $\Gamma_t(T_a)$ are shown in Figures 3.1 and 3.2, and the resulting slope at the points of inflection $E = E_\circ \pm \frac{\Gamma_t}{2\sqrt{3}}$ is shown in Figure 3.3. One can see that the optimum thickness is around $T_a \approx 4$, when the slope of the spectrum is steepest, assuming minimum $\mu_e$ and background.

3.2 <u>Broadened Lines</u>.

In general both the emission and the absorption line will be broadened by amounts differing from one source-absorber combination to another. As the broadening of the source and absorber lines are folded into the transmission spectrum, it is in general very difficult to separate the individual contributions, especially as it is not known a

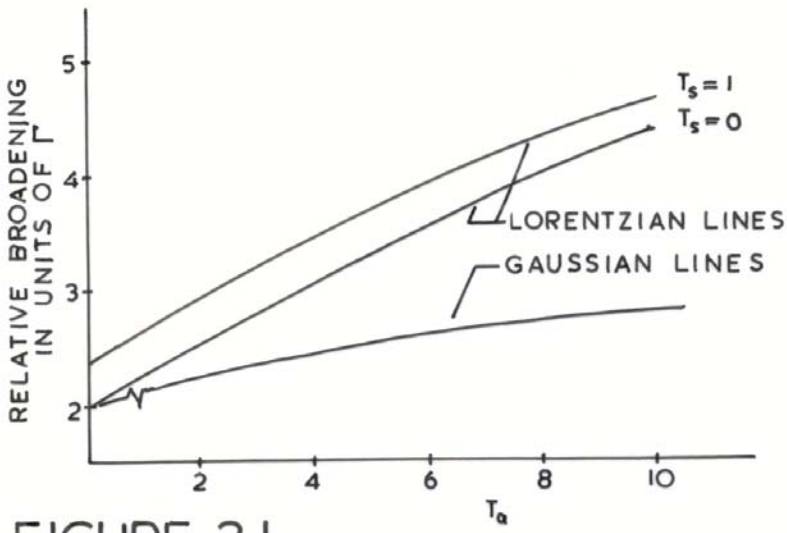


FIGURE 3.1

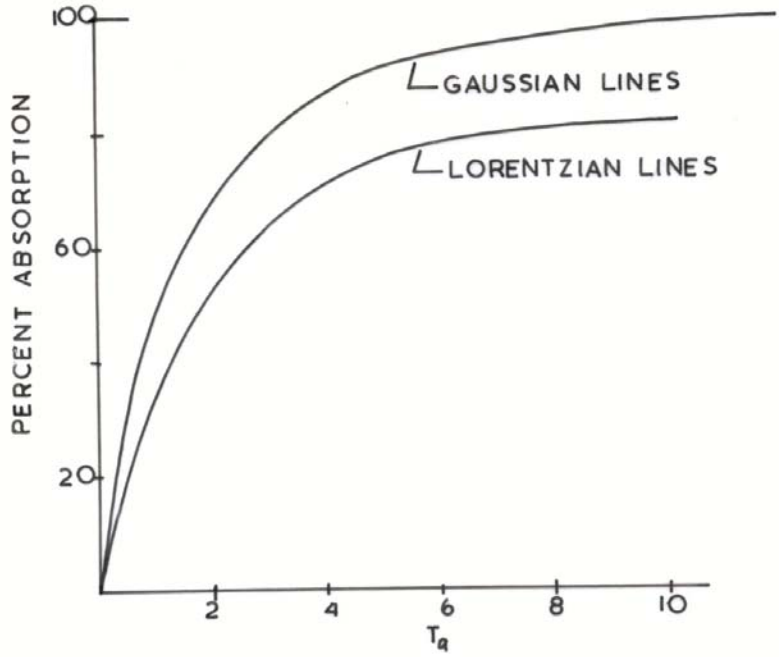


FIGURE 3.2

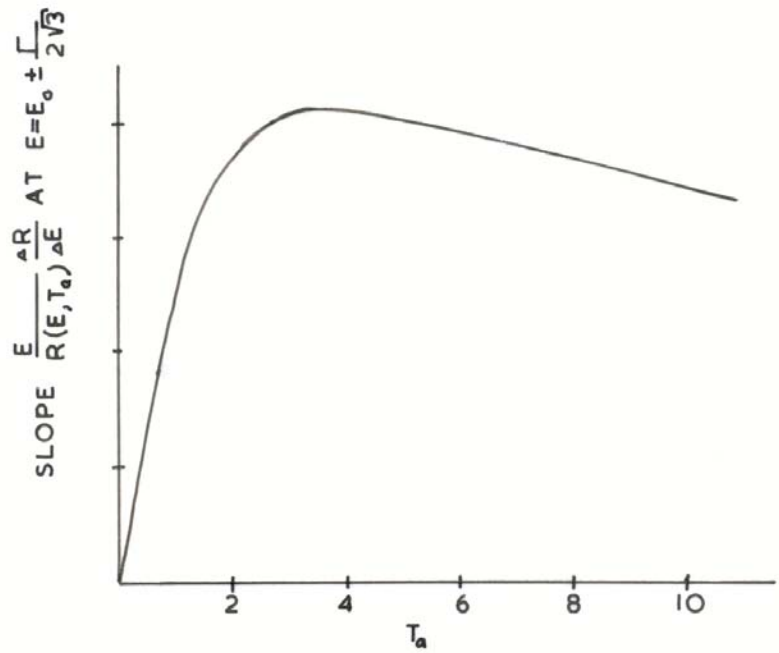
SLOPE $\frac{E}{R(E,T_a)}\frac{\Delta R}{\Delta E}$ AT $E=E_o \pm \frac{\Gamma}{2\sqrt{3}}$
2
4
6
8
10
$T_a$

FIGURE 3.3

priori if the broadening is of Lorentzian or of Gaussian character or possibly even of some other shape.

The difficulty arises from the fact that the convolution integral of two Lorentzians is different from that for two Gaussian functions. Equation 3.3.4 for $T_A << 1$ is essentially such an integral. Calculating the convolution integral using two Lorentzian lines of width $w_1$ and $w_2$, and similarly, two Gaussian lines of same width, the resulting width will be for the two cases

$$w_L = w_1 + w_2$$
$$w_G = (w_1^{\,2} + w_2^{\,2})^{1/2}$$

i.e., the Gaussian lines will not be broadened to the same extent as the Lorentzian will be. Margulies, et al., (1963) have calculated $R(S, T_a)$ and $\Gamma_t(T_a)$ for the case where both the emission and the absorption lines are pure Gaussian functions (see Figures 3.1, 3.2). The broadening is then much smaller, and the resonance dip, for a given value of absorber thickness, is much larger because of the preferential absorption at the centre of the emission line.

In general of course both these ideal cases are unrealistic, as in a practical situation, one would expect the lines to consist of a Gaussian distribution of Lorentzians. Such a line profile could be expresses by a Voigt integral (Posener, 1959)

$$H = \frac{1}{\pi}\int_{-\infty}^{\infty} \frac{e^{-x^2 a^2}\,dx}{1+(u-x)^2}$$

where $u = \dfrac{(E - E_\circ)}{\Gamma/2}$ and $\dfrac{1}{a} = \dfrac{\Gamma_G}{(\ln\ 2)^{1/2}\Gamma}$ expresses the Gaussian broadening. $\Gamma_G$ is the width of the Gaussian distribution. The convolution integral of two such integrals gives

another Voigt integral which represents the transmission spectrum for the case of a thin absorber.

Because of the admixture of Lorentzian and Gaussian components, the resulting broadening w of the line width would be $w_G$ ˆ w ˆ $w_L$ and in practice not enough parameters are available to extract the relative components without some simplifying assumptions.

One approach is to separate the transmission spectrum into its Lorentzian and Gaussian components and then to try to correlate the latter with either the source or the absorber parameters by, for example, increasing the thickness of a given absorber using the same source (Evans, 1968) or changing the source keeping the absorber parameters constant. In some cases one might find that the Gaussian contribution is predominantly due to either source or absorber. One can then subtract the Gaussian contribution and unfold the source-absorber lines in terms of Lorentzian widths.

Intuitively speaking, if the broadening is due to differences in the local environments, one might expect the resulting changes in the shifts and splittings to exhibit a Gaussian shape and furthermore expect them to be larger for substances where iron has been added as an impurity than for those where iron is chemically bonded, as in the case of the ferrocyanides. This has indeed been found when a 10 mCi $^{57}$Co (Pd) source, one of the rotor sources later to be described, was used in conjunction with a sodium ferrocyanide absorber of varying thickness (Evans, 1968).

3.3 Lorentz Broadened Lines.

O'Connor (1963) has derived the transmission spectrum for the case when the emission and absorption lines are both Lorentz broadened by amounts $1/k_s$ and $1/k_a$,

respectively. This approach could be used to treat some of the broadening mechanisms as a first approximation. As the calculation does give the resonance dip $R^1\left(O,T_a^1\right)$ and the line width $\Gamma_t^1(T_a)$ as a function of $k_s$ and $k_a$, the relationship between the various parameters emerges quite clearly.

Using a Lorentz approximation to expand the exponential in Equation 3.3.4, the resonance dip is given by

$$R^1(0,T_a^1)=\frac{(1+k)R\ (0,T_a^1)}{1+k\ \ k_a/k_s} \qquad ...3.8$$

where $T_a^1=k_aT_a$ and $k^{-1}$ is a parameter expressing the broadening due to the absorber thickness. $R^1(0,T_a^1)$ is shown in Figure 3.4 for the values $k_s/k_a=0.5,\ 1.0,\ 1.5$.

The transmission line width $\Gamma_t^1$ is found by evaluating the total transmission line shape

$$\Gamma_t^1=\Gamma\left(\frac{1}{k_s}+\frac{1}{k_a}\right)+0.27\Gamma T_a \text{ for } 0<T_a<5 \qquad ...3.9$$

This result reduces readily to the previous one (Equation 3.3.7) and gives surprisingly the same absorber broadening, even though the emission and the absorption lines have different widths than before.

Using the above two expressions for $\mathrm{R}^1$ and $\Gamma^1$, one can readily determine how the slope at the points of inflection of the resonance depends on the broadening of the individual lines. As the slope varies as $\mathrm{R}^1/\Gamma_t^1$ one can keep $\Gamma_t^1$ constant $\left(\Gamma_t^1=5\Gamma\right)$ and then plot $R^1\left(k_s,k_a,T_a\right)$ as a function of either $k_s$ or $k_a$ as shown in Figure 3.4. The solid lines give those values of $\mathrm{R}^1$ where $k_a$ is held constant and the dotted lines those for

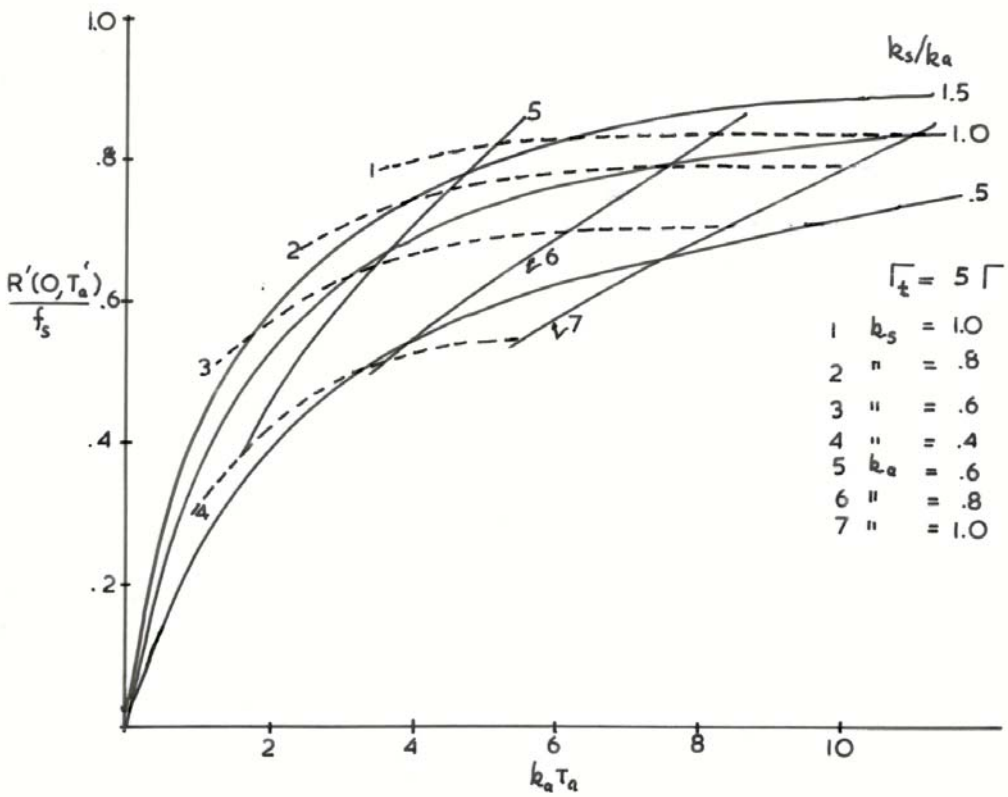
1.0
.8
.6
.4
.2
$\frac{R'(0,T_a')}{f_s}$
2
4
6
8
10
$k_a T_a$
$k_s/k_a$
1.5
1.0
.5
$\Gamma_t = 5\,\Gamma$
1 $k_s$ = 1.0
2 " = .8
3 " = .6
4 " = .4
5 $k_a$ = .6
6 " = .8
7 " = 1.0

FIGURE 3.4

constant $k_s$. As one might have expected, the largest value of $R^1$ occurs for $k_s = 1.0$ and decreases appreciably for increased source broadening, i.e., decreasing $k_s$. The resonance dip, however, does not depend very strongly on the broadening of the absorber line. For $k_s = 0.8$ and $k_a$ varying from 1.0 to 0.6 $R^1$ changes only by 2%.

Using these general criteria, one finds that, in order to obtain the largest possible slope, one must maximize $f_s$ and $k_s$ and choose values of $k_a T_a \square 4$.

4. <u>Recoilless Fraction</u>.

Several methods are available to measure the relative recoilless fraction of the source and absorber. An absolute measurement is more difficult, as it involves measuring a change in the beam intensity. Ideally one would need an absorber with unit absorption efficiency over the whole of the transmission line. An absorber made of a suitable combination of fluoroferrates best satisfies such criteria (Housley, et al., 1964) and gives $f_s$ directly by measuring $R_m$ after applying several corrections. The first accounts for the residual transmission at the centre of the absorption line and can be deduced by measuring the change in $R_m$ using a double black absorber. $\frac{\Delta R_M}{R_m}$ is of the order of 2%. The second correction compensates for the residual transmission at the wings and is less than 1% for $\Gamma_a \square 20\Gamma$.

An alternative correction method involves taking a transmission spectrum for both a single and a double black absorber, where the areas under the absorption peak, normalized to unit off-resonance-transmission, are $A_1$ and $A_2$, respectively. This gives (Duerdoth, 1965)

$$f_s = R_m \Big/ \left[ 1 - \left(1 - R_m\right) \frac{A_2}{A_1} \right]$$

This correction method is more accurate than the above, because it does not rely upon the knowledge of the line shapes of the source and absorber. It is, however, also more laborious.

Once the absolute value of $f_s$ for one source is known, that for all others can be directly found by using an identical absorber and determining the areas under the absorption peak, where then;

$$f_s^1 = f_s \, A^1 \big/ A$$

Similarly knowing $f_s$ and A for a thin absorber, one can determine $f_a$. The area under the absorption peak is

$$A = \int_{\circ}^{\infty} \left(1 - e^{-t\sigma_n(E)}\right) dE$$

and does not depend on the detailed shape of the emission line. This integral can be simply evaluated for the case of $Nf_a\sigma_{\circ} << 1$ when

$$A = \frac{\pi}{2} \; N\sigma_{\circ} f_s f_a \Gamma$$

Thus, for this special case, one can immediately obtain $f_a$. For greater thicknesses one has to evaluate the integral including higher order terms for the expansion of the exponential.

Another method for finding $f_a$ relies upon the assumptions made in Section 3.3.3. One can then deduce $f_a$ from the slope of $\Gamma_t(T_a)$ given by Equation 3.3.9.